CHIRALITY 16:637–641 (2004)

Absolute Configurational Determination of an All-*trans*-Retinal Dimer Isolated From Photoreceptor Outer Segments

NATHAN FISHKIN,[1] GENNARO PESCITELLI,[1] JANET R. SPARROW,[2]
KOJI NAKANISHI,[1]* AND NINA BEROVA[1]
[1]*Department of Chemistry, Columbia University, New York, New York*
[2]*Department of Ophthalmology, Columbia University, New York, New York*

ABSTRACT An all-*trans*-retinal (ATR) dimer (**1**) isolated from photoreceptor outer segments was found to have a stereogenic center at C13′ flanked by tetraene (295 nm) and hexaenal (438 nm) chromophores. Analytical chiral HPLC (Chiralcel OD) revealed that the isolated retinoid had formed in 13% enantiomeric excess. Using a combination of ^{1}H-^{1}H NOESY constraints, molecular modeling, and CD exciton coupling analysis, it was determined that the favored enantiomer was 13′(*R*). Three low-energy conformers of the 13′(S) model were found with MMFF/DFT and were used to calculate the CD spectrum of the ATR dimer (DeVoe method). The Boltzmann weighted spectrum was found to exhibit a positive exciton couplet, in excellent agreement with the experimental spectrum for the first eluted enantiomer. This further suggested that despite the large energy difference between the two interacting chromophores, the dominant source of optical activity in the CD spectrum is the nondegenerate exciton mechanism. *Chirality 16:637–641, 2004.*

KEY WORDS: exciton coupled circular dichroism; A2E; age related macular degeneration; chiral HPLC; fluorophore

There is mounting evidence indicating that the fluorescent granules that accumulate in retinal pigment epithelial (RPE) cells play an essential role in the death of these cells in macular degeneration. The only RPE lipofuscin fluorophores that have been characterized to date are A2E, its 13-(*Z*)-double bond isomer *iso*-A2E, and other minor isomers of A2E.[1–5] All of these compounds are generated through slow hydrolysis of the phosphate ester of A2-PE, the phosphatidyl-pyridinium bisretinoid that forms in photoreceptor outer segments. The synthesis of A2-PE occurs when molecules of all-*trans*-retinal (ATR), instead of undergoing reduction to all-*trans*-retinol, form conjugates with phosphatidylethanolamine through a series of random/nonenzyme-mediated reactions. The retinoid cycle is shown in Figure 1; illustrated also is the intersection between the visual cycle and the pathway by which A2-PE is formed.

The question remains as to whether other retinoid-derived fluorescent compounds accumulate in RPE in addition to A2E. We recently reported that at elevated ATR concentrations, a fluorescent bisretinoid adduct can form on lysine residues of rhodopsin in photoreceptor outer segments.[6] These findings may signify that fluorescent peptide fragments bearing A2-moieties become deposited in RPE cells. Additionally, we have isolated an enantiomerically enriched ATR dimer **1**[7,8] (Fig. 1), a bischromophoric condensation product of two molecules of ATR, from native photoreceptor outer segments. We propose that it forms under conditions of endogenous release of ATR from opsin (visual protein), and arises by divergence from the A2-PE biosynthetic pathway.[9,10] As this molecule possesses a stereogenic center at C13′, and its formation in photoreceptors is likely the result of general acid-base catalysis by membrane bound proteins in the outer segment, the possible enantiomeric excess of this isolated retinoid has been investigated and is reported here. Absolute configurational assignments of both enantiomers separated by chiral HPLC were made using a combination of NMR, molecular modeling, and the CD exciton chirality method.

EXPERIMENTAL

Determination of Percent Enantiomeric Excess

The ATR dimer **1** was resolved into enantiomers using analytical chiral HPLC (ChiralCel OD, 250 × 4.6 mm,

Contract grant sponsors: National Institutes of Health (NIH), NIH Vision; Contract grant numbers: GM-36564, GM-34509 (to K.N. and N.B.), EY-12951 (to J.R.S), EY 13933-03 (to N.F.).
Permanent address for Gennaro Pescitelli: University of Pisa, Dept. of Chemistry, Pisa, Italy.
*Correspondence to: K. Nakanishi, Department of Chemistry, Columbia University, New York, NY 10027. E-mail: kn5@columbia.edu
Received for publication 28 May 2004; Accepted 9 July 2004
DOI: 10.1002/chir.20084
Published online in Wiley InterScience (www.interscience.wiley.com).

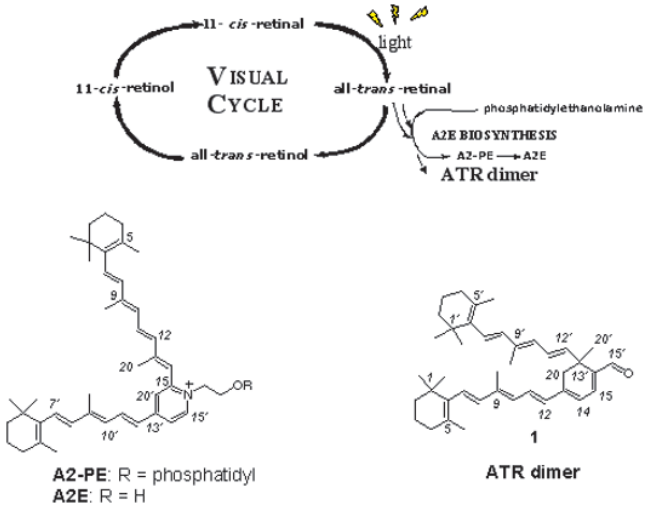

Fig. 1. Retinoid visual cycle. Light converts 11-*cis*-retinal to all-*trans*-retinal when covalently bound to the visual proteins called opsins. A dehydrogenase reduces the aldehyde to produce all-*trans*-retinol (vitamin A), which is then carried into the RPE cells where it is isomerized to 11-*cis*-retinol. Chaperone proteins then bring the *cis*-retinol back to the photoreceptors, where 11-*cis*-retinol dehydrogenase oxidizes it back to 11-*cis*-retinal to be used once again in the visual cycle. The point in the pathway where A2-PE, A2E, and ATR dimer are formed is shown along with their chemical structures. [Color figure can be viewed in the online issue, which is available at www.interscience.wiley.com.]

0.5 ml/min flow, 99.8/0.2 hexane/isopropanol, 430 nm detection, 10 μl injection). Injections were performed in triplicate and the integrated area of each peak was used to determine relative amounts of each enantiomer.

NMR Analysis

NOESY spectrum in $CDCl_3$ was acquired on a Bruker DMX400 in TPPI mode with the following parameters: spectral width 12 ppm, o1p 6.0 ppm, number of data points in F2 2K, and in F1 512 linear predicted to 1K and zero-filled to 2K, 32 scans per increment, mixing time 0.5 sec, relaxation delay 2 sec, acquisition time 0.18 sec, 90° pulse length, 7.2 μs processed with $\pi/2$ shifted sine-bell apodization. The sample was subjected to three freeze-pump-thaw cycles to remove oxygen prior to NOESY measurement.

Computational

Geometry optimization. A preliminary conformational search was performed with DFT (B3LYP/6-31G(d,p) level in $CHCl_3$) on a model of the ATR dimer **1** obtained by truncating the molecule at the C8′-C9′ and C8-C9 bonds. Structures with the tetraene substituent at C13′ in a pseudo-axial position were found globally more stable than the pseudo-equatorial isomers. Three rotamers relative to the C12′-C13′ torsion were evidenced.

A structure for the whole ATR dimer molecule **1,** with pseudo-axial tetraene at C13′, was built starting from the optimized model and subjected to C12′-C13′ dihedral scan with MMFF. Each rotamer thus obtained was further optimized with MMFF (convergence 0.0001) in $CHCl_3$. The three minimum energy conformers were finally evaluated with DFT B3LYP/6-31G(d,p) in $CHCl_3$. The DFT energies were used in the Boltzmann weight of the calculated CD spectra. MMFF calculations were run with MacroModel 7.1, DFT with Jaguar 4.1 (Schrödinger, Portland, OR) with default parameters and convergence criteria (unless otherwise noted).

CD calculations. The circular dichroic (CD) spectra were calculated according to the DeVoe method[11–13] for each of the three lowest energy conformers found using the above methods. Spectral parameters were taken from the UV-Vis absorption spectrum of the ATR dimer in $CHCl_3$ (1 kK = 10^3 cm^{-1}). Band I (C7…C15-C14′-C15 = O pentaenal chromophore): position λ = 436.7 nm (ν = 22.9 kK), dipolar strength 75.0 D^2, bandwidth $\Delta\nu$ = 4.5 kK; band II (C7′…C12′ triene chromophore): position λ = 302.1 nm (ν = 33.1 kK), dipolar strength 65.0 D^2, bandwidth $\Delta\nu$ = 7.5 kK. Transition dipoles were placed and oriented along the two chromophores (see Fig. 6). Transition dipole for band I was placed between C11-C13 and directed along C7-C13 direction, according to ZINDO/S-CI results on 2*E*,4*E*,6*E*,8*E*-undeca-2,4,6,8,10-pentenal (*s-cis* at C13-C14) within the dipole-velocity formalism.[14] DeVoe-type calculations were run with a Fortran program written by Hug and co-workers.[15] ZINDO calculations were run with Gaussian 03 (Pittsburgh PA) on DFT-optimized geometries (B3LYP/6-31G(d) level).

RESULTS AND DISCUSSION

A synthetic racemic sample of the ATR dimer was prepared by treating all-*trans*-retinal with NaH in dry THF at 0°C for 2 h (80% yield). This sample was initially applied to a ChiralCel AD column but could not be resolved into enantiomers even under a variety of solvent conditions. Eventually, a ChiralCel OD column, with a cellulose-based stationary phase, was found to give excellent baseline separation with ~17 min between the eluted enantiomers (Fig. 2, lower trace). In contrast to the racemic sample, the ATR dimer isolated from photoreceptor outer segments was found to have a larger integrated peak area for the second eluted enantiomer, corresponding to a 13% ee. The injections were repeated in triplicate and the standard

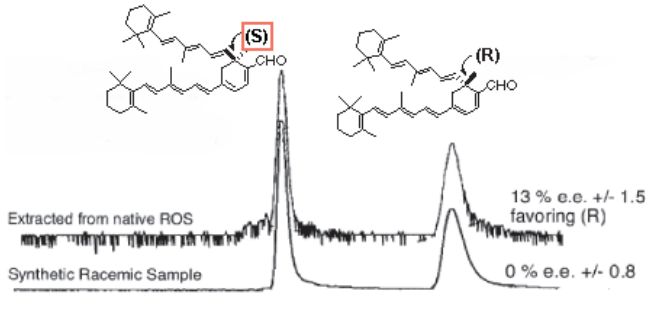

Fig. 2. Chiral HPLC separation of the two enantiomers of the ATR dimer on a Chiralcel OD column. The upper trace shows the separation carried out on the ATR dimer isolated from the $CHCl_3$/MeOH extracts of photoreceptor outer segments. The lower trace shows the separation of synthetic racemic material made under base-catalyzed conditions. The %ee's in each case are shown along with the standard error. The first eluted enantiomer had a retention time of 27.1 min, while the second one eluted at 44.8 min. [Color figure can be viewed in the online issue, which is available at www.interscience.wiley.com.]

errors (std. dev.) for %ee were calculated and are shown in Figure 2 for both synthetic racemic and naturally occurring ATR dimer.

The absorption spectrum of the ATR dimer (Fig. 3, bottom) is dominated by the $\pi-\pi^*$ transitions of the C5′-C12′ tetraene (λ = 289 nm, ϵ = 21,800 in $CHCl_3$) and C5-C15′ hexaenal (λ = 438 nm, ϵ = 25,000) chromophores, which may be regarded as isolated. Moreover, both eluted enantiomers gave a clear bisignate CD spectrum (Fig. 3, top, for the first eluted), therefore the exciton coupled CD method[16,17] could be conveniently applied to determine absolute configuration without the need for derivatization. A NOESY spectrum of the ATR dimer (in $CDCl_3$) revealed some close through-space ^1H-^1H interactions which were useful in determining the orientation of the two polyenes relative to the cyclohexadiene core (see arrows and numbering in Fig. 4). An NOE between 11-H and 20a-H (equatorial) indicates that the C5-C12 polyene moiety is fully conjugated to the cyclohexadiene ring. In addition, strong NOE pairs 20a-H/12′-H and 20b-H/20′-H suggest a pseudo-axial orientation for the C5′-C12′ tetraene, as shown in Figure 4. This observation that the 20′ methyl prefers a pseudo-equatorial position on the cyclohexadiene agrees with DFT calculations for a simplified model of **1** (see Computational section). It is also known from the literature on 5-substituted-1,3-cyclohexadienes[18,19] that bulky substituents (in the current case, the methyl group) tend to occupy the pseudo-equatorial position.[20] However, the main factor responsible for the present conformational preference may be entropic: the pseudo-axial tetraene chain at C13′ is fully allowed to rotate around the C12′-C13′ bond, while a pseudo-equatorial orientation would not allow for free rotation due to steric reasons (this is easily appreciated with a molecular model).

In addition, W-coupling (1 Hz) was observed between 20b-H and 12′-H, possibly suggesting a very small magnitude for the preferred dihedral angle around C11′-C12′-C13′-C20. In order to better evaluate the conformational situation relative to the C12′-C13′ torsion and its impact on the CD spectrum, a dihedral scan around C12′-C13′ (highlighted bonds in Fig. 5) was performed on the ATR dimer using MMFF and DFT calculations. Three low-energy rotamers of 0° (+0.4 kcal/mole, DFT energy), 120° (+0.0 kcal/mole), and 240° (+0.7 kcal/mole) were found (Fig. 5).

The CD spectrum was next calculated with the DeVoe method[11–13] for each of the three optimized conformers having the 13′(*S*) configuration and the pseudo-axial tetraene substituent at C13′. The electric transition mo-

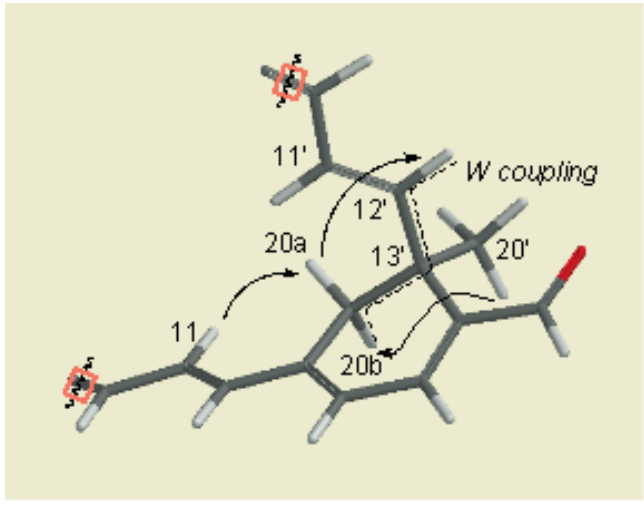

Fig. 4. Conformational analysis of the 13′(*S*) enantiomer of the ATR dimer. Arrows indicate proton pairs involved in strong NOEs. These close, through-space interactions were used to assign the C5′-C12′ polyene to the pseudo-axial position on the cyclohexadiene core. The dashed line indicates the pattern responsible for the observed W-coupling. [Color figure can be viewed in the online issue, which is available at www.interscience.wiley.com.]

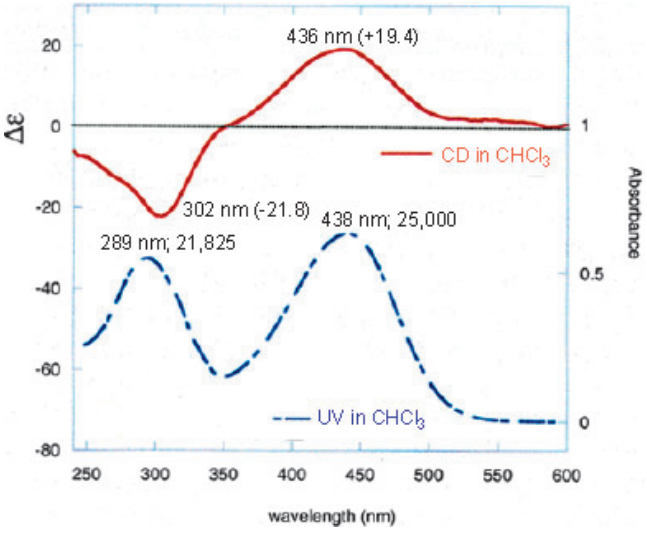

Fig. 3. Experimental CD and UV spectrum of the first eluted enantiomer (>99% ee) measured in $CHCl_3$. [Color figure can be viewed in the online issue, which is available at www.interscience.wiley.com.]

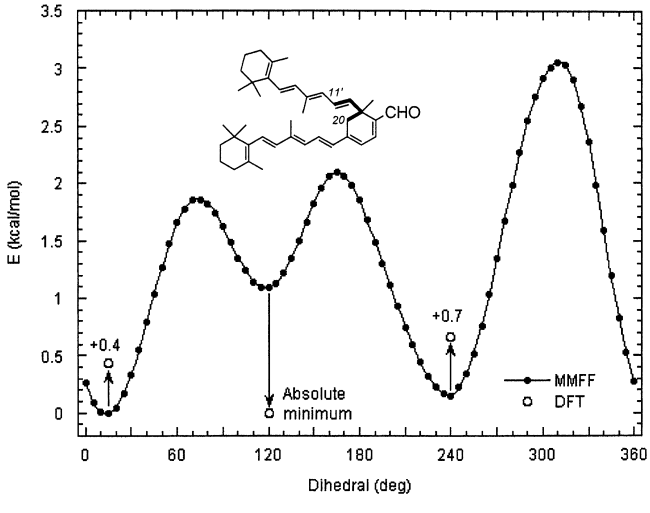

Fig. 5. Fully relaxed dihedral scan around C11′-C20 using MMFF. The graph of potential energy vs. dihedral angle (5° steps) is shown for the C5′-C12′ polyene in the equatorial position. Circles show DFT energies (B3LYP/6-31G(d,p) in $CHCl_3$) for the three minima.

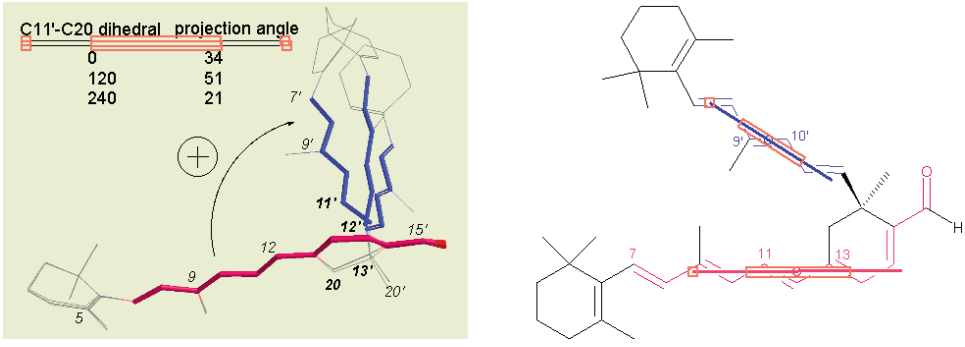

Fig. 6. Superimposition of the three low-energy conformers found for the (*S*) enantiomer. The C5-C15 polyene is highlighted in magenta and the C5′-C12′ polyene is shown in blue. The C11′-C20 dihedral along with the resulting interchromophoric projection angle are shown for each conformer. [Color figure can be viewed in the online issue, which is available at www.interscience.wiley.com.]

ment parameters were taken from the UV-vis absorption spectrum of **1** in $CHCl_3$; transition dipoles were placed in the middle of the two polyene chromophores and directed along their axes (see Computational section). Calculated CD spectra all exhibited a positive CD couplet; in fact, the chirality defined by the two chromophores is clearly positive in all cases for the 13′(*S*) configuration, although the interchromophoric distances and projection angle may vary (Fig. 6). As a consequence, the two conformers with 0° and 120° C11′-C20 dihedral gave roughly the same spectrum (amplitudes A = +42.0 and 39.5, respectively), while the 240° conformer led to a significantly reduced CD amplitude (A = +19.1). It is noteworthy that the most stable pseudo-equatorial conformer still gave a positive but very weak calculated CD couplet (A = +4.9); therefore, the contribution of the pseudo-equatorial isomer, if any, is negligible.

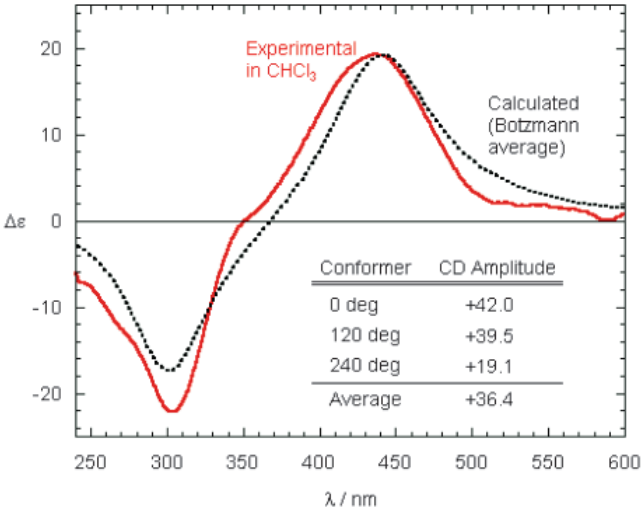

Fig. 7. Experimental (red solid line, in $CHCl_3$) and calculated CD spectrum (black dotted line and data) with DeVoe method on the (*S*) enantiomer. The black dotted spectrum is calculated as the Boltzmann-weighted average for the three lowest energy conformers found by MMFF/DFT modeling. CD amplitudes calculated for each conformer are also shown. [Color figure can be viewed in the online issue, which is available at www.interscience.wiley.com.]

The calculated DFT energies were then used to Boltzmann weight the calculated CD spectra. The weighted average spectrum is depicted in Figure 7 (dashed black line) along with the experimental CD for the first eluted enantiomer (>99% ee), showing a positive exciton couplet (302 nm $\Delta\epsilon$ = −21.8, 436 nm $\Delta\epsilon$ = +19.4, A = +41.2, in $CHCl_3$) due to a positive projection angle between the C5′-C12′ and C5-C15 chromophores (Fig. 6, see clockwise arrow). This observed CD spectrum is in excellent agreement with the DeVoe calculated spectrum for the ATR dimer having the (*S*) configuration. And since the second eluted compound gave a mirror image CD spectrum (not shown), we concluded that it was the (*R*) enantiomer of the ATR dimer. Absorption and CD spectra in hexane were also recorded, which are similar to those in $CHCl_3$, except that the long wavelength transition is considerably blue-shifted: band I, 422 nm, ϵ = 32,000, $\Delta\epsilon$ = +24.2 (first eluted); band II, 293 nm, ϵ = 29,440, $\Delta\epsilon$ = −22.9, A = +47.1.

Because the ATR dimer has been isolated from native photoreceptors in an enantiomerically enriched form favoring the 13′(*R*) configuration and has a fluorescent emission profile similar to A2E (emission max = 580 nm, 430 nm excitation, EtOH, 77K), we reasoned that the potential 100-fold increased sensitivity of FDCD[21] could be used to detect very low concentrations of this retinoid in eye tissue. However, a chiral sample of the ATR dimer did not give a detectable FDCD signal, presumably due to the negligible fluorescent quantum yield of the molecule at 25°C (F = 0.01).

CONCLUSION

CD exciton coupling analysis was used to determine the configuration of the enantiomer of the ATR dimer formed in excess in native eye tissue. The ATR dimer is formed in 13% ee, favoring the 13′(*R*) configuration. NOESY analysis combined with molecular modeling support a wedge-like structure for the ATR dimer (Fig. 6) with the C5′-C12′ polyene in the pseudo-axial position. The agreement between experimental and calculated CD demonstrates that the nondegenerate exciton mechanism is the leading source of optical activity, despite the remarkable energy difference between the two coupling chromophores (136 nm, 11,400 cm^{-1} in $CHCl_3$; 129 nm,

10,800 cm^{-1} in hexane, see Results). To the best of our knowledge, this molecule has the longest range exciton couplet of any natural product.

ACKNOWLEDGMENTS

We thank Profs. Yoshio Okamoto and Chiyo Yamamoto for invaluable assistance with chiral HPLC, as well as Dr. Katsunori Tanaka for assistance with FDCD.

LITERATURE CITED

1. Ben-Shabat S, Parish CA, Vollmer HR, Itagaki Y, Fishkin N, Nakanishi K, Sparrow JR. Biosynthetic studies of A2E, a major fluorophore of retinal pigment epithelial lipofuscin. J Biol Chem 2002;277:7183–7190.
2. Eldred GE, Lasky MR. Retinal age pigments generated by self-assembling lysosomotropic detergents. Nature 1993;361:724–726.
3. Liu J, Itagaki Y, Ben-Shabat S, Nakanishi K, Sparrow JR. The biosynthesis of A2E, a fluorophore of aging retina, involves the formation of the precursor, A2-PE, in the photoreceptor outer segment membrane. J Biol Chem 2000;275:29354–29360.
4. Mata NL, Weng J, Travis GH. Biosynthesis of a major lipofuscin fluorophore in mice and humans with ABCR-mediated retinal and macular degeneration. Proc Natl Acad Sci U S A 2000;97:7154–7159.
5. Parish CA, Hashimoto M, Nakanishi K, Dillon J, Sparrow JR. Isolation and one-step preparation of A2E and iso-A2E, fluorophores from human retinal pigment epithelium. Proc Natl Acad Sci U S A 1998;95: 14609–14613.
6. Fishkin N, Jang Y-P, Itagaki Y, Sparrow JR, Nakanishi K. A2-rhodopsin: a new fluorophore isolated from photoreceptor outer segments. Org Biomol Chem 2003;1:1101–1105.
7. Asato AE, Watanabe C, Li XY, Liu RSH. The proline and b-lactoglobulin mediated asymmetric self-condensation of b-ionylideneacetaldehyde, retinal and related compounds. Tetrahedron Lett 1992;33;3105–3108.
8. Verdegen PJE, Monnee MCF, Mulder PPJ, Lugtenburg J. Condensation of all-E-retinal. Tetrahedron Lett 1997;38:5355–5358.
9. Fishkin NE, Pescitelli G, Itagaki Y, Berova N, Allikmets R, Nakanishi K, Sparrow JR. Isolation and characterization of a novel RPE fluorophore: An all-trans-retinal dimer. Invest Ophthalmol Vis Sci 2004; 45E-abstract:1803.
10. Sakai N, Decatur J, Nakanishi K, Eldred GE. Ocular age pigment "A2-E": an unprecedented pyridinium bisretinoid. J Am Chem Soc 1996;118:1559–1560.
11. Di Bari L, Pescitelli G, Reginato G, Salvadori P. Conformational investigation of two isomeric chiral porphyrins: a convergent approach with different techniques. Chirality 2001;13:548–555.
12. Pescitelli G, Gabriel S, Wang Y, Fleischhauer J, Woody RW, Berova N. Theoretical analysis of the porphyrin-porphyrin exciton interaction in circular dichroism spectra of dimeric tetraarylporphyrins. J Am Chem Soc 2003;125:7613–7628.
13. Rosini C, Zandomeneghi M, Salvadori P. Coupled oscillator calculations of circular dichroism intensities: structural applications in organic chemistry. Tetrahedron: Asymm 1993;4:545–554.
14. Mason SF. Molecular optical activity and the chiral discriminations. Cambridge, UK: Cambridge University Press; 1982. p 66–68.
15. Cech CL, Hug W, Tinoco Jr I. Polynucleotide circular dichroism calculations: use of an all-order classical coupled oscillator polarizability theory. Biopolymers 1976;15:131–152.
16. Harada N, Nakanishi K. Circular dichroic spectroscopy — exciton coupling in organic stereochemistry. Mill Valley, CA: University Science Books; 1983.
17. Nakanishi K, Berova N. Exciton chirality method: principles and applications. In: Nakanishi K, Berova N, Woody RW, editors. Circular dichroism — principles and applications. New York: Wiley-VCH; 2000. p 337–382.
18. Lightner DA, Gurst JE. Organic conformational analysis and stereochemistry. In: Lightner DA, editor. Circular dichroism spectroscopy. New York: John Wiley & Sons; 2000. p 400–405.
19. Rabideau PW, Sygula A. In: Rabideau PW, editor. Conformational analysis of cyclohexenes, cyclohexadienes, and related hydroaromatic compounds. New York: Wiley-VCH; 1989. p 71–73.
20. Eliel EL, Wilen SH, Mander LN. Stereochemistry of organic compounds. New York: John Wiley & Sons; 1994. p 695–700.
21. Nehira T, Parish CA, Jockusch S, Turro N, Nakanishi K, Berova N. Fluorescence-detected exciton-coupled circular dichroism: scope and limitation in structural studies of organic molecules. J Am Chem Soc 1998;121;8681–8691.